Original Article

Synthesis and phototoxicity of isomeric 7,9-diglutathione pyrrole adducts: Formation of reactive oxygen species and induction of lipid peroxidation

Liang Ma [a,*], Hengqiang Zhao [a], Qingsu Xia [a], Lining Cai [b], Peter P. Fu [a,*]

[a] Division of Biochemical Toxicology, National Center for Toxicological Research, Jefferson, AR 72079, USA
[b] Biotranex LLC, Monmouth Junction, NJ 08852, USA

ARTICLE INFO

ABSTRACT

Pyrrolizidine alkaloids (PAs) are hepatotoxic, genotoxic, and carcinogenic in experimental animals. Because of their widespread distribution in the world, PA-containing plants are probably the most common poisonous plants affecting livestock, wildlife, and humans. Upon metabolism, PAs generate reactive dehydro-PAs and other pyrrolic metabolites that lead to toxicity. Dehydro-PAs are known to react with glutathione (GSH) to form 7-GSH-(+/−)-6,7-dihydro-7-hydroxy-1-hydroxymethyl-5*H*-pyrrolizine (7-GS-DHP) *in vivo* and *in vitro* and 7,9-diGS-DHP *in vitro*. To date, the phototoxicity of GS-DHP adducts has not been well studied. In this study, we synthesized 7-GS-DHP, a tentatively assigned 9-GS-DHP, and two enantiomeric 7,9-diGS-DHP adducts by reaction of dehydromonocrotaline with GSH. The two 7,9-diGS-DHPs were separated by high performance liquid chromatography (HPLC) and their structures were characterized by ^{1}H nuclear magnetic resonance (NMR) and ^{1}H–^{1}H correlation spectroscopy (COSY) NMR spectral analysis. Photoirradiation of 7-GS-DHP, 9-GS-DHP, and the two 7,9-diGS-DHPs as well as dehydromonocrotaline, dehydroheliotrine, and the 7-R enantiomer of DHP (DHR), by UVA light at 0 J/cm^2, 14 J/cm^2, and 35 J/cm^2 in the presence of a lipid, methyl linoleate, all resulted in lipid peroxidation in a light dose-responsive manner. The levels of lipid peroxidation induced by the two isomeric 7,9-diGS-DHPs were significantly higher than that by 7-GS-DHP and 9-GS-DHP. When 7,9-diGS-DHP was irradiated in the presence of sodium azide (NaN$_3$), the level of lipid peroxidation decreased; lipid peroxidation was enhanced when methanol was replaced by deuterated methanol. These results suggest that singlet oxygen is a product induced by the irradiation of 7,9-diGS-DHP. When irradiated in the presence of superoxide dismutase (SOD), the level of lipid peroxidation decreased, indicating that lipid peroxidation is also mediated by superoxide. These results indicate that lipid peroxidation is mediated by

reactive oxygen species (ROS). These results suggest that 7,9-diGS-DHPs are phototoxic, generating lipid peroxidation mediated by ROS.

1. Introduction

More than 660 pyrrolizidine alkaloids (PAs) and PA N-oxides have been identified in > 6000 plant species distributed worldwide. To date, about half of these phytochemicals have been determined to be hepatotoxic, and many of them are genotoxic and tumorigenic in experimental animals, suggesting that PA-containing plants are probably the most common poisonous plants affecting livestock, wildlife, and humans [1–9].

PAs require metabolism to generate reactive pyrrolic metabolites to exert cytotoxicity, genotoxicity, and tumorigenicity [1,3–5,10–16]. The primary pyrrolic metabolites, dehydro-PAs, are highly unstable and reactive, and readily react with water in the medium to form (±)-6,7-dihydro-1-hydroxymethyl-5H-pyrrolizine (DHP) as a secondary pyrrolic metabolite [1]. Both dehydro-PAs and DHP can bind to cellular proteins and DNA leading to DHP-protein and DNA adducts that are responsible for PA-induced toxicity in liver and other tissues such as lung, kidney, and skin [1,9]. In addition to skin cancer, PAs also cause secondary (hepatogenous) photosensitization [17,18].

Dehydro-PAs and DHP as well as the 7R enantiomer of DHP (DHR) also react with glutathione (GSH) to form 7-glutathionyl-DHP (7-GS-DHP) in vitro and in vivo [19–24] and 7,9-diGS-DHP in vitro [22–24]. Fashe et al [25] recently identified (3H-pyrrolizin-7-yl)methanol, a newly found reactive metabolite, from human liver microsomal metabolism of the tumorigenic PAs, retrorsine, lasiocarpine, and senkirkine. Reaction of (3H-pyrrolizin-7-yl)methanol with GSH also generated both 7-GS-DHP and 7,9-diGS-DHP adducts in vitro [25].

Although 7-GS-DHP has long been considered a detoxified metabolite [1,5,26], we recently found that 7-GS-DHP can bind to calf thymus DNA to form the same set of DHP-DNA adducts that have been shown to be biomarkers of PA exposure and potential biomarkers of PA-induced tumorigenicity [27]. Under similar experimental conditions, 7,9-diGS-DHP did not react with calf thymus DNA to form DHP-DNA adducts [27].

We have been interested in studying PA-induced phototoxicity [17,18]. We found that upon UVA irradiation, a series of dehydro-PAs (dehydromonocrotaline, dehydroriddelliine, dehydroretrorsine, dehydrosenecionine, dehydroseneciphylline, dehydrolasiocarpine, and dehydroheliotrine) and 7-GS-DHP adducts all induce lipid peroxidation mediated by reactive oxygen species (ROS) in a light dose-responsive manner, while the parent PAs and PA N-oxides did not induce lipid peroxidation [17,18]. In the present study, we synthesized the two isomeric 7,9-diGS-DHP adducts, determined their phototoxicity under UVA light irradiation, and established that the induced lipid peroxidation was mediated by ROS in a level similar to those from dehydro-PAs.

2. Materials and methods

2.1. Chemicals

Monocrotaline, GSH, formic acid, sodium azide (NaN_3), and superoxide dismutase (SOD) were purchased from Sigma-Aldrich (St. Louis, MO, USA). Dimethylformamide (DMF), acetonitrile, potassium carbonate, chloroform, and diethyl ether were purchased from Fisher Scientific (Pittsburg, PA, USA). Heliotrine was obtained from Accurate Chemical & Scientific Corporation (Westbury, NY, USA). Dehydromonocrotaline and dehydroheliotrine were prepared by dehydrogenation of monocrotaline and heliotrine, respectively, in chloroform with o-chloranil following the procedure reported previously [17,28]. C18 (particle size: 56.1 μm) was obtained from Waters (Milford, Massachusetts, USA).

2.2. Light sources

The UVA light box consisting of four UVA lamps (National Biologics, Twinsburg, OH, USA) was custom made [29–31]. The light spectral irradiance of the light box was determined using an Optronics OL754 spectroradiometer (Optronics Laboratories, Orlando, FL, USA). The light dose of the UVA light box, with the maximum emission between 340 nm and 355 nm, was routinely measured using a Solar Light PMA-2110 UVA detector (Solar Light Inc., Philadelphia, PA, USA). As reported previously [29,30], the light intensities at wavelengths < 320 nm (UVB light) and > 400 nm (visible light) are approximately two orders of magnitude lower than the maximum in the 340–355 nm spectral region.

In this study, the UVA-irradiation doses were 14 J/cm^2 and 35 J/cm^2, which were obtained by approximately 46 minutes and 115 minutes of exposure, respectively, at the dose rate of 5 mW/cm^2 [17]. UVA 10 J/cm^2 equates to about 2 hours of exposure at noon on sunny summer days, based upon observation of UVA intensity of 5.4 mW/cm^2 in Paris, France, in July [32].

2.3. Synthesis of 7-GS-DHP and 9-GS-DHP adducts

7-GS-DHP and 9-GS-DHP adducts were synthesized following our previously reported procedure for the synthesis of 7-GS-DHP with modification [27]. GSH (13 mg, 42 μmol), dissolved in 70 μL phosphate-buffered saline

(0.1M, pH 7.4), was added to a solution of dehydromonocrotaline (20 mg, 62 μmol) in 1 mL DMF. The reaction mixture was stirred at ambient temperature for 2 hours and then quenched with 10 mL phosphate-buffered saline. The products were separated by high performance liquid chromatography (HPLC). HPLC conditions: Phenomenex Luna C18 (2) column, 250 × 4.6 mm, monitored at 220 nm, with flow rate at 1 mL/min; isocratic program: 3% acetonitrile in 0.01% formic acid and ammonia solution (pH 8).

2.4. Synthesis of 7,9-diGS-DHP adducts

Dehydromonocrotaline (20 mg, 62 μmol), dissolved in 300 μL DMF, was directly added to a solution of GSH (100 mg, 325 μmol) in 600 μL deionized water (pH 5) at 4°C. The reaction mixture was sonicated at ambient temperature for 30 minutes and then the reddish precipitate was removed by Centrifugation (4000g). The product, contained in the two peaks, was separated by HPLC [Phenomenex Luna C18 (2) column, 250 mm × 10 mm] using 20% methanol in 0.1% formic acid water solution with flow rate at 3 mL/min. The solvent was removed from the two products under reduced pressure; 18 mg 7,9-diGS-DHP-1 and 18 mg 7,9-diGS-DHP-2 (each 4% yield) were obtained. The purity was checked by HPLC [Phenomenex Luna C18 (2) column, 250 mm × 4.6 mm].

2.5. Photoirradiation of 7-GS-DHP, 9-GS-DHP, and 7,9-diGS-DHPs with UVA light in the presence of methyl linoleate

Experiments were conducted using a solution of 100mM methyl linoleate and 0.1mM 7-GS-DHP, 9-GS-DHP, or 7,9-diGS-DHP in methanol. Samples were placed in a UV-transparent cuvette and irradiated with 0 J/cm^2, 14 J/cm^2, or 35 J/cm^2 of UVA light. After irradiation, the methyl linoleate hydroperoxide products were separated by HPLC using a Prodigy 5 μm Octadecylsilyl (ODS) column (250 mm × 4.6 mm, Phenomenex, Torrance, CA, USA) eluted isocratically with 10% water in methanol (v/v) at 1 mL/min. The level of lipid peroxidation was determined by HPLC and was quantified by monitoring HPLC peak areas at 235 nm followed by conversion to concentrations based on the molar extinction coefficient (at 235 nm) [29–31].

2.6. Photoirradiation of dehydromonocrotaline, dehydroheliotrine, and DHR with UVA light in the presence of methyl linoleate

For comparison of phototoxicity with other PA pyrrolic metabolites, photoirradiation of 0.1mM dehydromonocrotaline, dehydroheliotrine, and DHR was conducted in parallel with 7-GS-DHP, 9-GS-DHP, and 7,9-diGS-DHP adducts.

2.7. UVA light-induced lipid peroxidation by 7,9-diGS-DHP in the presence of a free radical scavenger or an enhancer

The experiments were carried out as described above, in the presence of NaN$_3$, or SOD. The concentration of SOD was

200 U/mL and the concentration of NaN$_3$ was 20mM. Photoirradiation of 7,9-diGS-DHP in CH$_3$OH containing deuterium methanol (CH$_3$OD) was studied similarly.

2.8. Liquid chromatography-electrospray-mass spectrometry/mass spectrometry analysis of GSH-DHP adducts

GSH-DHP adducts were analyzed by the liquid chromatography-electrospray-mass spectrometry/mass spectrometry (LC-ES-MS/MS) method. The Shimadzu Prominence HPLC system consisted of a CBM-20A system controller, two LC-20AD pumps, a SIL-20AC HT autosampler, an SPD-20A UV/VIS detector (Shimadzu Scientific Instrument, Columbia, MD, USA), and an automated switching valve (TPMV, Rheodyne, Cotati, CA, USA). The HPLC was coupled with an AB Sciex 4000 QTrap LC/MS/MS system (AB Sciex, Foster City, CA, USA) and a Turbo V ion source. Desolvation temperature was set at 450°C and nitrogen was used as curtain gas, nebulizer gas, heater gas, and collision gas. The samples were acquired in positive ion spray mode using MS full scan and enhanced product ion scan. The ion spray voltage was 5000 V; the ion source gas 1 was set to 60 and gas 2 was set to 50. The declustering potential was 50 V and the collision energy was 25 eV for enhanced product ion [33].

Each sample (10–30 μL) was loaded onto a reverse phase column (ACE 3 C18, 4.6 mm × 150 mm, 3 μm, MAC-MOD Analytical Inc., Chadds Ford, PA, USA), with a water/acetonitrile gradient at 0.7 mL/min. The column chamber temperature was set to 40°C. The mobile phases were A: 2mM ammonium acetate in water containing 0.1% formic acid; and B: acetonitrile containing 0.1% formic acid. The initial 0% organic mobile phase was held for 5 minutes, then increased linearly to 25% over 30 minutes. The organic mobile phase was increased from 25% to 35% in 10 minutes followed by washing column at 95% for 3 minutes then back to the initial condition [33].

2.9. Statistical analysis

Data are expressed as means ± standard deviation ($n = 3$). One-way analysis of variance followed by pairwise-comparisons using Dunnett's t tests was used to determine the significance of difference in photoinduced hydroperoxidation between samples with substrates and a control sample (methyl linoleate only). The difference was considered statistically significant when $p < 0.05$.

3. Results

3.1. Synthesis of 7-GS-DHP, 9-GS-DHP, and 7,9-diGS-DHP adducts

Following our previously published synthetic procedure for the synthesis of 7-GS-DHP with modification [27], reaction of dehydromonocrotaline with GSH at a 1:0.67 molar ratio was conducted for 2 hours and the resulting reaction products were separated by HPLC (Fig. 1A). LC/MS/MS spectral analysis of the reaction mixture indicated three mono-GS-DHP adducts, each having an [M − H$_2$O + H]$^+$ ion
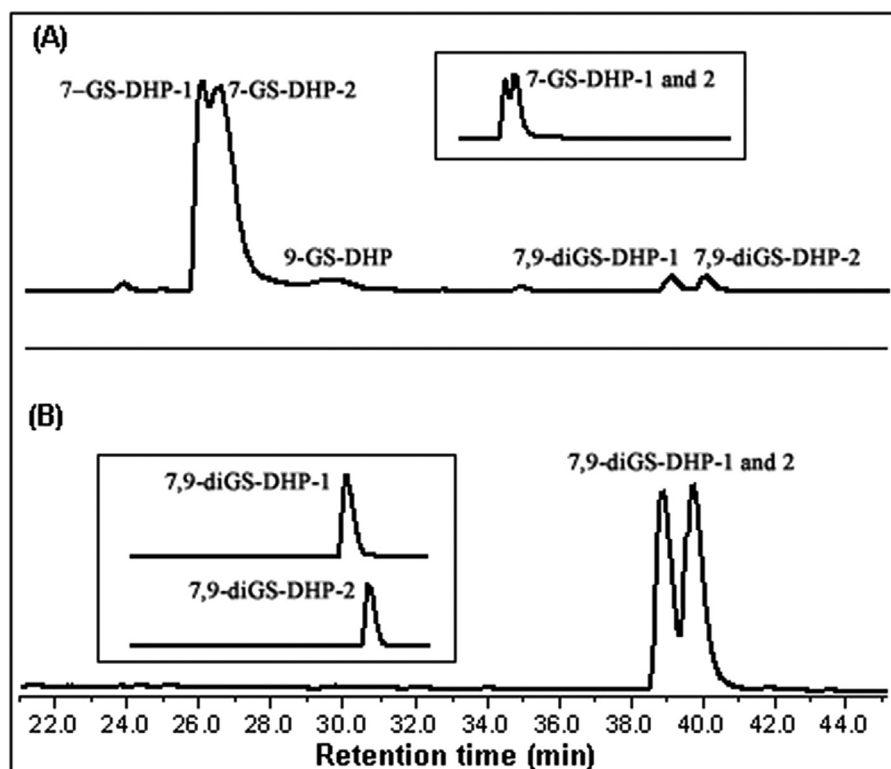
Fig. 1 − High performance liquid chromatography (HPLC) profiles of: (A) 7-GS-DHP-1, 7-GS-DHP-2, 9-GS-DHP, 7,9-diGS-DHP-1, and 7,9-diGS-DHP-2 formed from reaction of glutathione (GSH) with dehydromonocrotaline; and (B) 7,9-diGS-DHP-1 and 7,9-diGS-DHP-2 adducts upon further HPLC separation. Conditions: Phenomenex Luna C18 (2) column, 250 mm × 4.6 mm, monitored at 220 nm, with flow rate at 1 mL/min; gradient program: 0–60 minutes, 5–15% acetonitrile in 0.01% formic acid water solution. 7-GS-DHP = 7-glutathione-(±)-6,7-dihydro-1-hydroxymethyl-5H-pyrrolizine; 9-GS-DHP = 9-glutathione-(±)-6,7-dihydro-1-hydroxymethyl-5H-pyrrolizine; 7,9-diGS-DHP-1 = 7,9-diglutathione-(±)-6,7-dihydro-1-hydroxymethyl-5H-pyrrolizine-1; 7,9-diGS-DHP-2 = 7,9-diglutathione-(±)-6,7-dihydro-1-hydroxymethyl-5H-pyrrolizine-2; 7-GS-DHP-1 = 7-glutathione-(±)-6,7-dihydro-1-hydroxymethyl-5H-pyrrolizine-1 and 7-GS-DHP-2 = 7-glutathione-(±)-6,7-dihydro-1-hydroxymethyl-5H-pyrrolizine-2..

at m/z 425, an $[M + H]^+$ ion at m/z 443, and an $[M + Na]^+$ ion at m/z 465 (Fig. 2), and two diGS-DHP adducts, each having an $[M - H_2O + H]^+$ ion at m/z 733 and an $[M - H_2O + Na]^+$ ion at m/z 755 (Fig. 3). 7-GS-DHP-1 and 7-GS-DHP-2 were the predominant adducts (a total of 12% yield) and the two 7,9-diGS-DHPs were the minor adducts (a total of 0.5% yield; Fig. 4). In addition to mass spectrometric analysis, the structures of 7-GS-DHP-1 and 7-GS-DHP-2 adducts were confirmed by their ^1H nuclear magnetic resonance (NMR) spectral profiles similar to those previously reported by Robertson et al [34], Lin et al [35], and Tamta et al [24].

A third GS-DHP isomer that eluted at 29.5 minutes in Fig. 1 was a minor product produced in a 0.5% yield (Fig. 4). It was highly unstable and could not be isolated in a sufficient amount for structural characterization by NMR spectral analysis. Based on its molecular weight and the understanding that a pyrrolic compound has two reactive electrophilic sites at C7 and C9 positions [1], this third GS-DHP product was tentatively assigned as 9-GS-DHP.

The reaction of dehydromonocrotaline with GSH at a 1:0.67 molar ratio produced 7,9-diGS-DHP-1 and 7,9-diGS-DHP-2 adducts (Fig. 1A) only in a 0.5% yield (Fig. 4). When five-fold excess GHS was used for reaction, 7,9-diGS-DHP-1 and 7,9-diGS-DHP-2 adducts were generated in a 6% yield (Fig. 1B and 4). In addition to mass spectrometric analysis (Fig. 3), their structures were confirmed by ^1H NMR (Fig. 5) and ^1H–^1H correlation spectroscopy (COSY) NMR (Fig. 6) spectral analysis, as well as by comparison of their ^1H NMR spectra with that of 7-GS-DHP (Fig. 5; Table 1). As shown in Table 1, the spectra of 7,9-DiGS-DHP-1 and 7,9-diGS-DHP-2 adducts are highly similar to that of 7-GS-DHP, with the exception that the chemical shift of the two C-9 protons at 4.46–4.57 ppm in 7-GS-DHP are shifted upfield to 3.7–3.92 ppm, a > 0.65 ppm upfield shift, in both 7,9-diGS-DHP-1 and 7,9-diGS-DHP-2 (Table 1). This upfield shift is consistent with the observation by Robertson et al [34] and contributed to the different shielding characteristics and electronegativity of substituents from an oxygen atom (such as the C7 hydroxyl group of DHR) compared to a sulfur atom in the formation of 7-GS-DHP and
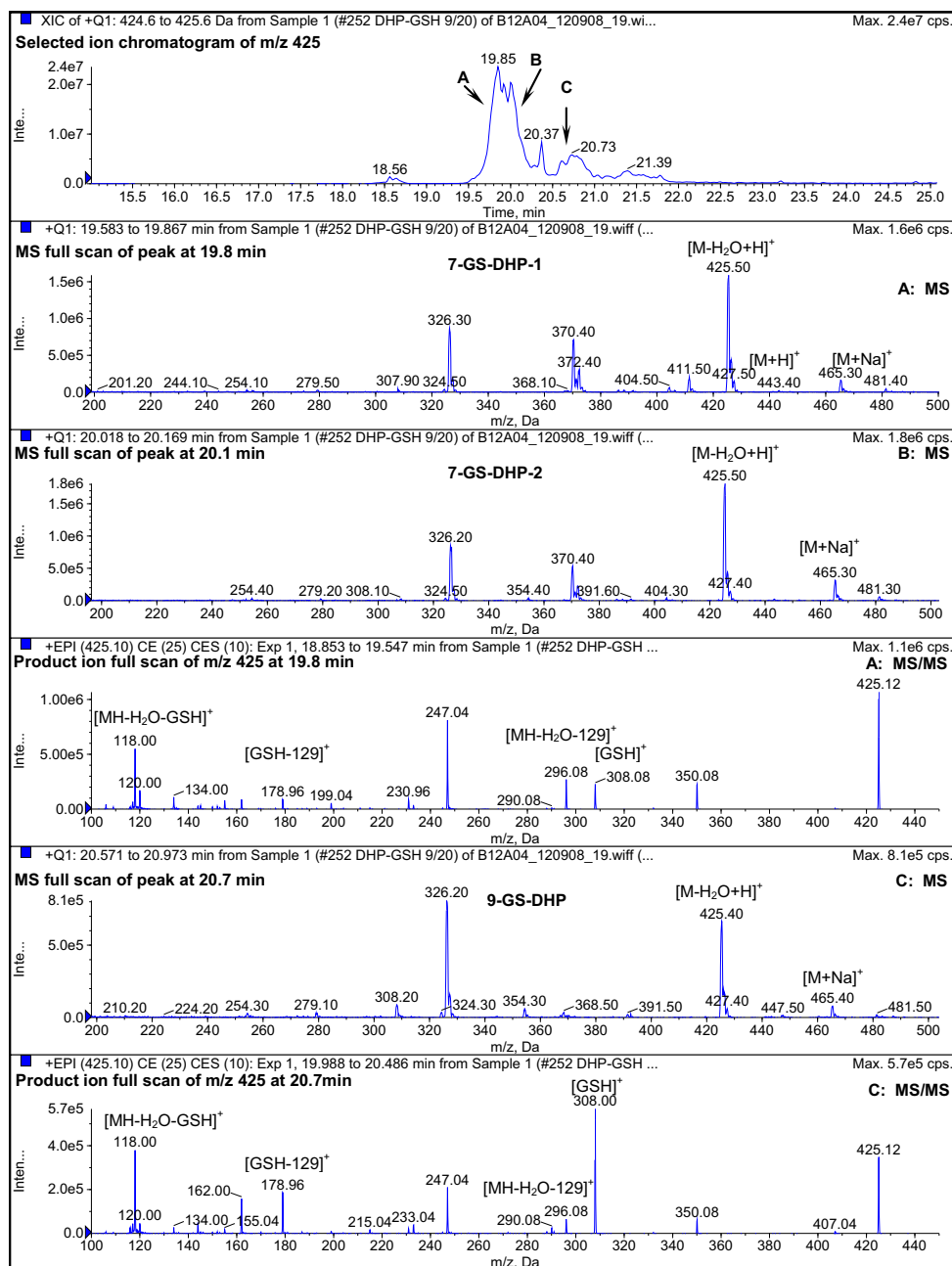
Fig. 2 – Liquid chromatography (LC)/UV/mass spectrometry (MS) spectral data of 7-GS-DHP adducts (A, B) and 9-GS-DHP adduct (C). GSH = glutathione; MH = molecular weight.

7-cysteine-DHP from reactions of DHR with GSH and cysteine.

3.2.   Photoirradiation of 7-GS-DHP, 9-GS-DHP, 7,9-diGSH-DHP-1, and 7,9-diGSH-DHP-2 with UVA light in the presence of methyl linoleate.

7-GS-DHP, 9-GS-DHP, 7,9-diGS-DHP-1, and 7,9-diGS-DHP-2 in methanol were individually photoirradiated with 0 J/cm², 14 J/cm², or 35 J/cm² UVA light in the presence of methyl linoleate. For comparison, photoirradiation of methyl linoleate alone, and dehydromonocrotaline, dehydroheliotrine, and DHR in the presence of methyl linoleate was also conducted. The

extent of lipid peroxide formed by irradiation was measured by calculation of the amount of methyl linoleate hydroperoxide based on the HPLC peak areas detected at 235 nm [29–31,36].

The results indicated that the UVA irradiation of these GS-DHP adducts all generated lipid peroxidation significantly higher than that of the control (Fig. 7A). Similarly, photoirradiation of dehydromonocrotaline, dehydroheliotrine, and DHR also generated lipid peroxidation (Fig. 7B). The results shown in Table 2 indicate that the levels of lipid peroxidation are in the order: 7,9-diGS-DHP-2 ~ 7,9-diGS-DHP-1 ~ dehydromonocrotaline ~ dehydroheliotrine > 7-GS-DHP ~ 9-GS-DHP ~ DHR > control [17].
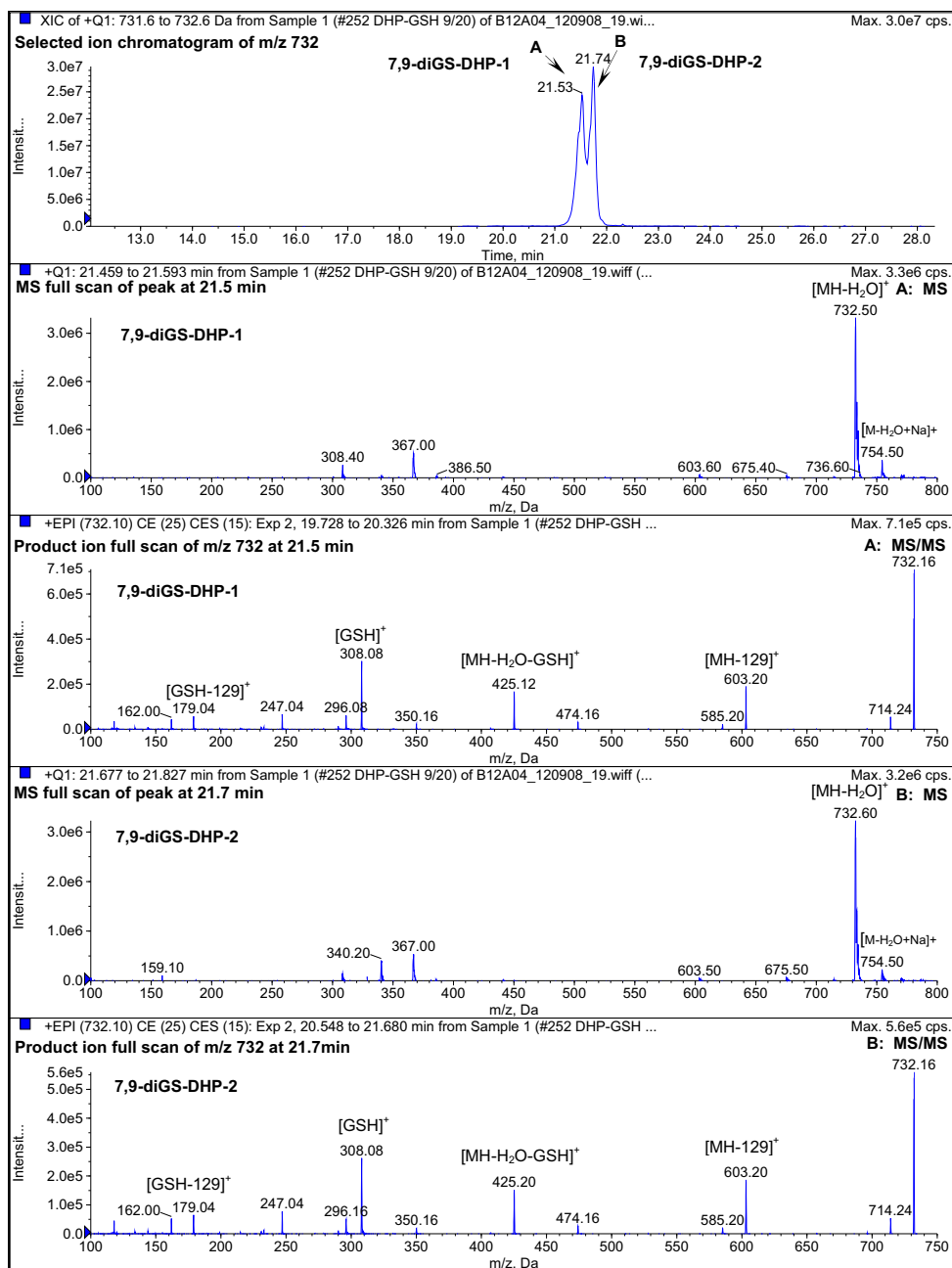
Fig. 3 – Liquid chromatography (LC)/UV/mass spectrometry (MS) spectra of 7,9-diGS-DHP adducts. GSH = glutathione; MH = molecular weight.
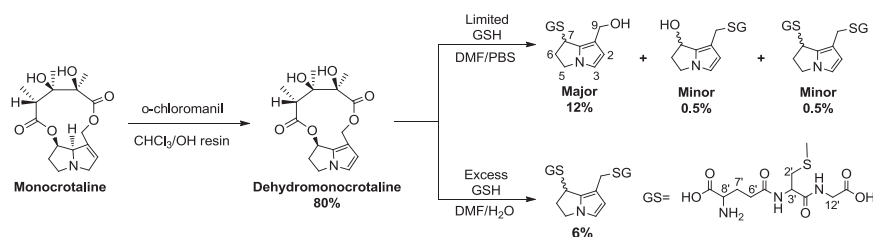

Fig. 4 – Synthesis of glutathione-(±)-6,7-dihydro-1-hydroxymethyl-5H-pyrrolizine (GSH-DHP) adducts from reaction of dehydromonocrotaline and GSH.
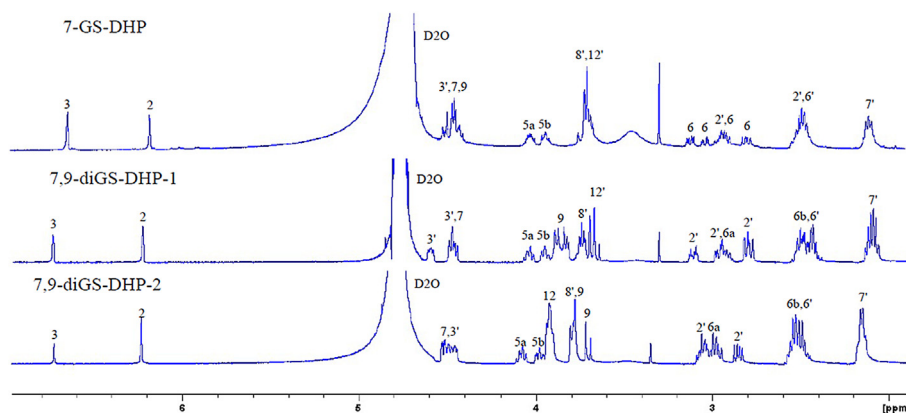
Fig. 5 — ^{1}H nucleic magnetic resonance (NMR) spectra of 7-GS-DHP, 7,9-diGS-DHP-1 and 7,9-diGS-DHP-2 measured in D$_2$O. The absolute stereochemistry depicted at C7 is arbitrary.
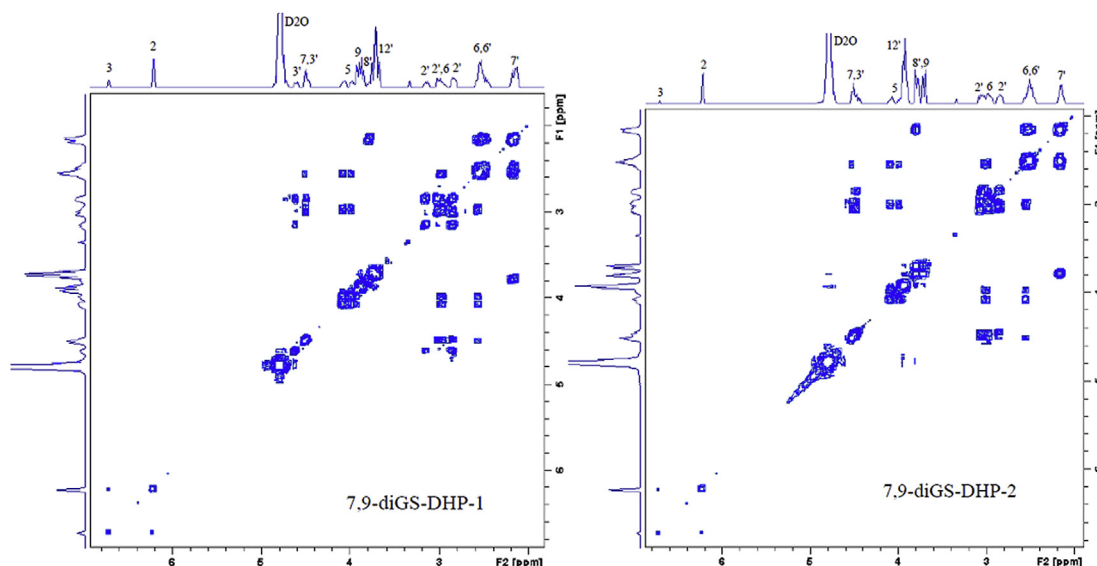

Fig. 6 — ^{1}H—^{1}H correlation spectroscopy (COSY) spectra of 7,9-diGS-DHP-1 and 7,9-diGS-DHP-2 adducts measured in D$_2$O. The absolute stereochemistry depicted at C7 is arbitrary.

Table 1 — Proton nuclear magnetic resonance (NMR) spectroscopic data (500 MHz) of the necine base in the synthetically prepared 7-GS-DHP, 7,9-DiGS-DHP-1, and 7,9-DiGS-DHP-2 adducts measured in D$_2$O (δ in ppm, J in Hz).

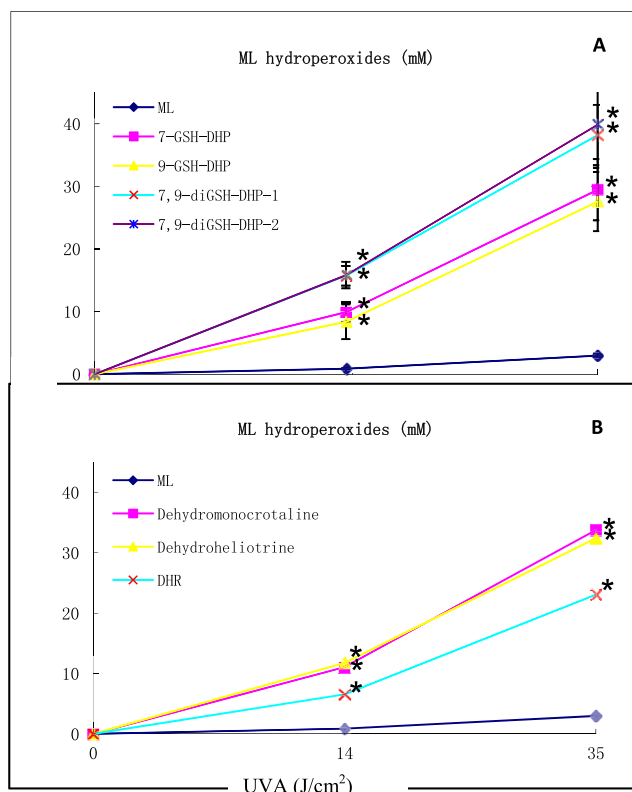| Assignment	7-GS-DHP	7,9-DiGS-DHP-1	7,9-DiGS-DHP-2
H2	6.24 (1H, d, 2.6)	6.22 (1H, d, 2.6)	6.22 (1H, d, 2.6)
H3	6.71 (1H, d, 2.6)	6.73 (1H, d, 2.6)	6.73 (1H, d, 2.6)
H5a	4.07 (1H, m)	4.08 (1H, m)	4.08 (1H, m)
H5b	3.99 (1H, m)	3.99 (1H, m)	3.98 (1H, m)
H6a	2.98 (1H, m)	2.96 (1H, m)	2.97 (1H, m)
H6b	2.55 (1H, m)	2.57 (1H, m)	2.55 (1H, m)
H7	4.46—4.57 (1H, m)	4.50 (1H, m)	4.52 (1H, m)
H9a	4.46—4.57 (1H, m)	3.92 (1H, m)	3.79 (1H, m)
H9b	4.46—4.57 (1H, m)	3.87 (1H, m)	3.70 (1H, m)

Fig. 7 – Induction of lipid peroxidation by photoirradiation of: (A) 0.1 mM 7-GS-DHP, 9-GS-DHP, 7,9-diGS-DHP-1, and 7,9-diGS-DHP-2; and (B) dehydromonocrotaline, dehydroheliotrine, and DHR (the 7R-enantiomer of DHP) in methanol in the presence of methyl linoleate (ML) with UVA light at light doses of 0 J/cm², 14 J/cm², and 35 J/cm², respectively, in methanol in the presence of ML, respectively. Data are expressed as mean ± standard deviation (n = 3). The levels of peroxidation were measured by high performance liquid chromatography monitored at 235 nm. * Significant difference from control (ML only; $p < 0.05$).

3.3. UVA light-induced lipid peroxidation by 7,9-diGS-DHP in the presence of a free radical scavenger or enhancer

The effect on the levels of lipid peroxide induced from photoirradiation of 7,9-diGS-DHP-1 and 7,9-diGS-DHP-2 with UVA light in the presence of NaN₃, SOD (superoxide scavenger), or CH₃OD (enhancement of singlet oxygen lifetime) was also investigated. The concentration of NaN₃ and SOD was 20mM and 200 U/mL, respectively, and the amount of CH₃OD was 10% in methanol.

NaN₃ can effectively scavenge both singlet oxygen ($^1O_2$) and hydroxyl radical (·OH) [37,38]. Consequently, use of NaN₃ alone cannot determine whether or not singlet oxygen is involved in peroxidation of methyl linoleate by photoirradiation of 7,9-diGS-DHP-1 or 7,9-diGS-DHP-2. Since singlet oxygen has a longer half-life in CH₃OD than in methanol [37], use of both NaN₃ and CH₃OD provides a reliable approach for

Table 2 – UVA photoirradiation of 0.1mM GS-DHP conjugates in the presence of methyl linoleate. Data are expressed as mean ± standard deviation (n = 3).

Chemical	Methyl linoleate hydroperoxide (mM)	
	UVA 14 J/cm²	UVA 35 J/cm²
Methyl linoleate	0.87 ± 0.11	2.98 ± 0.30
7-GS-DHP	9.90 ± 1.54	29.47 ± 4.90
9-GS-DHP [a]	8.37 ± 2.77	27.57 ± 4.74
7,9-diGS-DHP-1	15.75 ± 1.57	39.19 ± 4.80
7,9-diGS-DHP-2	15.83 ± 2.13	39.86 ± 6.91
Dehydromonocrotaline	11.05 ± 1.30	33.76 ± 1.52
Dehydroheliotrine	11.77 ± 0.45	32.38 ± 0.55
DHR [b]	6.57 ± 0.50	23.09 ± 3.15

DHR = 7-R enantiomer of DHP.
[a] Structure tentatively assigned as 9-GS-DHP was based on UV-visible and mass spectral analysis.
[b] Possibly due to DHR decomposition during the experiment, in our previous study [17], UVA photoirradiation of DHR did not induce lipid peroxidation at a level significantly higher than in the control.
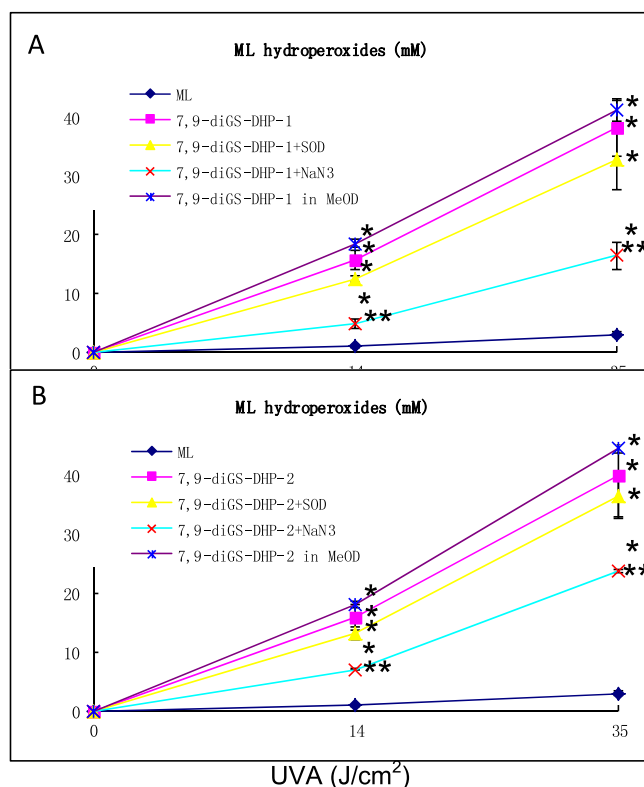

Fig. 8 – Effects of deuterated methanol, NaN₃, and superoxide dismutase (SOD) on peroxidation of methyl linoleate initiated by UVA photoirradiation of 0.1mM (A) 7,9-diGS-DHP-1 and (B) 7,9-diGS-DHP-2. The levels of peroxidation were measured by high performance liquid chromatography (HPLC) monitored at 235 nm. Data are expressed as mean ± standard deviation (n = 3).
* Significant difference from negative control ($p < 0.05$).
** Significant difference between the groups with and without a free radical scavenger or an enhancer ($p < 0.05$).

determining whether or not singlet oxygen is involved in lipid peroxidation.

The results shown in Fig. 8A clearly indicate that lipid peroxidation was inhibited by NaN_3 and SOD (all with $p \leq 0.05$), but was enhanced by the presence of CH_3OD ($p \leq 0.05$). These results suggest that peroxidation of methyl linoleate initiated by UVA irradiation of 7,9-diGS-DHP-1 is mediated by free radicals. In addition, the inhibition of lipid peroxidation by NaN_3 and enhancement by CH_3OD indicate that singlet oxygen is involved in peroxidation.

UVA irradiation of 7,9-diGS-DHP-2 obtained nearly identical results, e.g., inhibition of lipid peroxidation by NaN_3 and SOD, and enhancement of lipid peroxidation by CH_3OD (Fig. 8B).

4. Discussion

The synthesis of 7-GS-DHP and a mixture of the two isomeric 7,9-diGS-DHP adducts was previously reported [24,27,35]; however, the reaction yields of these products were not determined and the two 7,9-diGS-DHP adducts were not separated for the structural identification. In the present study, we repeated the synthesis with modification, provided the reaction yields, separated 7,9-diGS-DHP-1 and 7,9-diGS-DHP-2 adducts by HPLC, and elucidated their structures by mass, ^{1}H NMR, and COSY NMR spectral analysis. A mono-GS-DHP, tentatively assigned as 9-GS-DHP, was also produced from the reaction. Compared with the geometric isomer 7-GS-DHP, this tentatively assigned 9-GS-DHP is highly unstable and could not be collected in a sufficient quantity for structural characterization by NMR spectral analysis. By contrast, although both 7,9-diGS-DHP-1 and 7,9-diGS-DHP-2 also possess a glutathionyl group at the C9 position of the necine base, they are relatively highly stable. The reasons for the marked difference in stability among these compounds warrant investigation.

In the present study, we demonstrate that upon UVA irradiation, 7,9-diGS-DHP-1, 7,9-diGS-DHP-2, 7-GS-DHP, and 9-GS-DHP all generate ROS that leads to the induction of lipid peroxidation. 7,9-DiGS-DHP adducts are metabolites formed *in vitro* [24,25,35]. We recently reported that 7-GS-DHP is a potential DNA reactive metabolite of PAs, capable of reacting with calf thymus DNA to produce DHP-DNA adducts, which are biomarkers of PA exposure and potential biomarkers of PA-induced liver tumors [27]. We also found that 7,9-diGS-DHP did not react with calf thymus DNA [27], indicating that 7,9-diGS-DHP may be biologically inactive. In the present paper, we report the first demonstration that 7,9-diGS-DHP adducts are chemically phototoxic and capable of generating lipid peroxidation upon UVA irradiation. These results suggest that 7,9-diGS-DHP-1 and 7,9-diGS-DHP-2 can potentially cause skin damage in humans.

The phototoxicity potency of 7-GS-DHP, 9-GS-DHP, 7,9-diGS-DHP-1, and 7,9-diGS-DHP-2 was about the same level as that of dehydro-PAs, including dehydromonocrotaline, dehydroriddelliine, dehydroretrorsine, dehydrosenecionine, dehydroseneciphylline, dehydrolasiocarpine, and dehydroheliotrine [17]. The lipid peroxidation generated by UVA irradiation of 7,9-diGS-DHP-1 and 7,9-diGS-DHP-2 was

mediated by ROS. The involvement of singlet oxygen in UVA light-induced lipid peroxidation by both 7,9-diGS-DHP-1 and 7,9-diGS-DHP-2 was determined by the inhibition effect by NaN_3 and the enhancement by deuterated methanol (Fig. 8). The inhibition of lipid peroxidation by SOD suggested that lipid peroxidation was mediated by superoxide (Fig. 8). The results of this mechanistic study are very similar to those we previously reported for UVA photoirradiation of dehydro-PAs [17].

The overproduction of ROS and lipid peroxidation in humans is associated with many age-related diseases including cancer, atherosclerosis, ischemia, inflammation, liver injury, and aging [39,40]. Skin is the organ that can concomitantly be exposed to sunlight and PAs, PA N-oxides, and possibly their metabolites, such as dehydro-PAs, DHP, and pyrrole-GSH adducts. The results from this and previous studies suggest that when 7-GS-DHP, 7,9-diGS-DHP, dehydro-PAs, and DHP are present in the skin, they can induce ROS and lipid peroxidation, and lead to skin damage.

Conflicts of interest

All contributing authors declare no conflicts of interest. This article is not an official US FDA guidance or policy statement. No official support or endorsement by the US FDA is intended or should be inferred. The authors declare no competing financial interest.

Acknowledgments

REFERENCES

[1] Mattocks AR. Chemistry and toxicology of pyrrolizidine alkaloids. London: Academic Press; 1986.

[2] Huxtable RJ. Human health implications of pyrrolizidine alkaloids and herbs containing them. In: Cheeke PR, editor. Toxicants of plant origin, vol. 1. Boca Raton: CRC Press; 1989. p. 41—86.

[3] Fu PP, Chou MW, Xia Q, Yang YC, Yan J, Doerge DR, Chan PC. Genotoxic pyrrolizidine alkaloids and pyrrolizidine alkaloid N-oxides — mechanisms leading to DNA adduct formation and tumorigenicity. J Environ Sci Health, Part C 2001;19:353—85.

[4] Fu PP, Yang YC, Xia Q, Chou MW, Cui YY, Lin G. Pyrrolizidine alkaloids-tumorigenic components in Chinese herbal medicines and dietary supplements. J Food Drug Anal 2002;10:198—211.

[5] Fu PP, Xia Q, Lin G, Chou MW. Pyrrolizidine alkaloids-genotoxicity, metabolism enzymes, metabolic activation, and mechanisms. Drug Metab Rev 2004;36:1—55.

[6] Fu PP, Chou MW, Churchwell M, Wang Y, Zhao Y, Xia Q, Gamboa da Costa G, Marques MM, Beland FA, Doerge DR. High-performance liquid chromatography electrospray ionization tandem mass spectrometry for the detection and quantitation of pyrrolizidine alkaloid-derived DNA adducts in vitro and in vivo. Chem Res Toxicol 2010;23:637–52.

[7] Roeder E. Medicinal plants in China containing pyrrolizidine alkaloids. Pharmazie 2000;55:711–26.

[8] Edgar JA, Roeder E, Molyneux RJ. Honey from plants containing pyrrolizidine alkaloids: a potential threat to health. J Agric Food Chem 2002;50:2719–30.

[9] Edgar JA, Molyneux RJ, Colegate SM. Pyrrolizidine alkaloids: potential role in the etiology of cancers, pulmonary hypertension, congenital anomalies, and liver disease. Chem Res Toxicol 2015;28:4–20.

[10] International Programme on Chemical Safety (IPCS). Health and Safety Criteria Guide 26: Pyrrolizidine Alkaloids Health and Safety Guide. Geneva, Switzerland: World Health Organization; 1989.

[11] Yang YC, Yan J, Doerge DR, Chan PC, Fu PP, Chou MW. Metabolic activation of the tumorigenic pyrrolizidine alkaloid, riddelliine, leading to DNA adduct formation in vivo. Chem Res Toxicol 2001;14:101–9.

[12] Fu PP, Xia Q, Chou MW, Lin G. Detection, hepatotoxicity, and tumorigenicity of pyrrolizidine alkaloids in Chinese herbal plants and herbal dietary supplements. J Food Drug Anal 2007;15:400–15.

[13] Chen T, Mei N, Fu PP. Genotoxicity of pyrrolizidine alkaloids. J Appl Toxicol 2010;30:183–96.

[14] Zhao Y, Xia Q, Gamboa da Costa G, Yu H, Cai L, Fu PP. Full structure assignments of pyrrolizidine alkaloid DNA adducts and mechanism of tumor initiation. Chem Res Toxicol 2012;25:1985–96.

[15] Xia Q, Chou MW, Kadlubar FF, Chan PC, Fu PP. Human liver microsomal metabolism and DNA adduct formation of the tumorigenic pyrrolizidine alkaloid, riddelliine. Chem Res Toxicol 2003;16:66–73.

[16] Xia Q, Zhao Y, Von Tungeln LS, Doerge D, Lin G, Cai L, Fu PP. Pyrrolizidine alkaloids-derived DNA adducts as a common biological biomarker of pyrrolizidine alkaloid-induced tumorigenicity. Chem Res Toxicol 2013;26:1384–96.

[17] Zhao Y, Xia Q, Yin JJ, Lin G, Fu PP. Photoirradiation of dehydropyrrolizidine alkaloids–formation of reactive oxygen species and induction of lipid peroxidation. Toxicol Lett 2011;205:302–9.

[18] Wang C-C, Xia Q, Li M, et al. Metabolic activation of pyrrolizidine alkaloids leading to phototoxicity and photogenotoxicity in human HaCaT keratonicytes. J Environ Sci Health, Part C 2014;32:362–84.

[19] Lame MW, Morin D, Jones AD, Segall HJ, Wilson DW. Isolation and identification of a pyrrolic glutathione conjugate metabolite of the pyrrolizidine alkaloid monocrotaline. Toxicol Lett 1990;51:321–9.

[20] Buhler DR, Miranda CL, Kedzierski B, Reed RL. Mechanisms for pyrrolizidine alkaloid activation and detoxification. Adv Exp Med Biol 1991;283:597–603.

[21] Mattocks AR, Croswell S, Jukes R, Huxtable RJ. Identity of a biliary metabolite formed from monocrotaline in isolated, perfused rat liver. Toxicon 1991;29:409–15.

[22] Reed RL, Miranda CL, Kedzierski B, Henderson MC, Buhler DR. Microsomal formation of a pyrrolic alcohol glutathione conjugate of the pyrrolizidine alkaloid senecionine. Xenobiotica 1992;22:1321–7.

[23] Lin G, Cui YY, Hawes EM. Microsomal formation of a pyrrolic alcohol glutathione conjugate of clivorine. Firm evidence for the formation of a pyrrolic metabolite of an otonecine-type pyrrolizidine alkaloid. Drug Metab Dispos 1998;26:181–4.

[24] Tamta H, Pawar RS, Wamer WG, Grundel E, Krynitsky AJ, Rader JI. Comparison of metabolism-mediated effects of pyrrolizidine alkaloids in a HepG2/C3A cell-S9 co-incubation system and quantification of their glutathione conjugates. Xenobiotica 2012;42:1038–48.

[25] Fashe MM, Juvonen RO, Petsalo A, Rahnasto-Rilla M, Auriola S, Soininen P, Vepsäläinen J, Pasanen M. Identification of a new reactive metabolite of pyrrolizidine alkaloid retrorsine: (3H-pyrrolizin-7-yl)methanol. Chem Res Toxicol 2014;27:1950–7.

[26] Yan CC, Huxtable RJ. Relationship between glutathione concentration and metabolism of the pyrrolizidine alkaloid, monocrotaline, in the isolated, perfused liver. Toxicol Appl Pharmacol 1995;130:132–9.

[27] Xia Q, Ma L, He X, Cai L, Fu PP. 7-Glutathione pyrrole adduct: a potential DNA reactive metabolite of pyrrolizidine alkaloids. Chem Res Toxicol 2015;28:615–20.

[28] Yang YC, Yan J, Churchwell M, Beger R, Chan P, Doerge DR, Fu PP, Chou MW. Development of a ^{32}P-postlabeling/HPLC method for detection of dehydroretronesine-derived DNA adducts in vitro and in vivo. Chem Res Toxicol 2001;14:91–100.

[29] Cherng S-H, Xia Q, Blankenship LR, Freeman JP, Wamer WG, Howard PC, Fu PP. Photodecomposition of retinyl palmitate in ethanol by UVA light – formation of photodecomposition products, reactive oxygen species, and lipid peroxides. Chem Res Toxicol 2005;18:129–38.

[30] Xia Q, Yin JJ, Cherng S-H, Wamer WG, Boudreau M, Howard PC, Fu PP. UVA photodecomposition of retinyl palmitate – formation of singlet oxygen and superoxide, and their role in induction of lipid peroxidation. Toxicol Lett 2006;163:30–43.

[31] Chiang HM, Yin JJ, Xia Q, Zhao Y, Fu PP, Wen K-C, Yu H. Photoirradiation of azulene and guaiazulene–formation of reactive oxygen species and induction of lipid peroxidation. J Photochem Photobiol A Chem 2010;211:123–8.

[32] Jeanmougin M, Civatte J. Dosimetry of solar ultraviolet radiation. Daily and monthly changes in Paris. Ann Dermatol Venereol 1987;114:671–6.

[33] Jiang X, Wang S, Zhao Y, Xia Q, Cai L, Sun X, Fu PP. Absolute configuration, stability, and interconversion of 6,7-dihydro-7-hydroxy-1-hydroxymethyl-5H-pyrrolizine valine adducts and their phenylthiohydantoin derivatives. J Food Drug Anal 2015;23:318–26.

[34] Robertson KA, Seymour JL, Hsia M-T, Allen JR. Covalent interaction of dehydroretronecine, a carcinogenic metabolite of the pyrrolizidine alkaloid monocrotaline, with cysteine and glutathione. Cancer Res 1977;37:3141–4.

[35] Lin G, Cui YY, Hawes EM. Characterization of rat liver microsomal metabolites of clivorine, an hepatotoxic otonecine-type pyrrolizidine alkaloid. Drug Metab Dispos 2000;28:1475–83.

[36] Herreño-Sáenz D, Xia Q, Fu PP. UVA photoirradiation of methylated benzo[a]pyrene and benzo[e]pyrene leading to induction of lipid peroxidation. Int J Environ Res Public Health 2007;4:145–52.

[37] Basu-Modak S, Tyrrell RM. Singlet oxygen: a primary effector in the ultraviolet A/near-visible light induction of the human heme oxygenase gene. Cancer Res 1993;53:4505–10.

[38] Sortino S, Condorelli G, de Guidi G, Giuffrida S. Molecular mechanism of photosensitization XI. Membrane damage and DNA cleavage photoinduced by enoxacin. Photochem Photobiol 1998;68:652–9.

[39] Floyd RA, West M, Hensley K. Oxidative biochemical markers: clues to understanding aging in long-lived species. Exp Gerontol 2001;36:619–40.

[40] Stadtman ER, Berlett BS. Reactive oxygen-mediated protein oxidation in aging and disease. Chem Res Toxicol 1997;10:485–94.